Theoretical Study of the Atmospheric Reaction between Dimethyl Sulfide and Chlorine Atoms

Stella M. Resende* and Wagner B. De Almeida

Laboratório de Química Computacional e Modelagem Molecular, Departamento de Química, ICEx, UFMG, Belo Horizonte, MG, 31270-901, Brazil

Received: June 10, 1997; In Final Form: October 9, 1997[⊗]

The atmospheric reaction between dimethyl sulfide and chlorine atoms was studied theoretically at the UQCISD-(T)/DZP//UMP2/DZP level of calculation. The molecular structure and relative stability of several possible adducts between these two species were investigated. We have obtained four additional adducts bound through the carbon and hydrogen atoms, besides the one already known, where the intermolecular bond occurs between the chlorine atom and the lone pair of the sulfur atom. These complexes are very weakly bound, and only one of them can lead to reaction. Four possible channels for the reaction were investigated, and we have found that the $(CH_3)_2SCl$ adduct and the products of hydrogen abstraction, CH_3SCH_2 and HCl, are the most important ones. The reaction $\Delta G°$ values for these two channels are negative, −5.63 −5.33 kcal/mol, respectively, and the rate constants very large, because these reactions proceed without energy barrier. However, under atmospheric conditions, the estimate of the equilibrium constants indicates that the first channel will reach the equilibrium faster than the abstraction channel, and the concentration of the $(CH_3)_2SCl$ adduct will be very small. The formation of the CH_3S and CH_3Cl products is considerably hindered. Despite the fact that this pathway is spontaneous ($\Delta G° = -12.13$ kcal/mol), it has a high activation free energy barrier ($\Delta G^{‡} = 31.45$ kcal/mol), and the rate constant was estimated as 2.1×10^{-30} cm^3 molecule^{-1} s^{-1}. The channel that leads to the CH_3SCl and CH_3 products is conditional to the formation of the $(CH_3)_2SCl$ adduct. However, its high activation free energy ($\Delta G^{‡} = 29.25$ kcal/mol) and instability in relation to reactants ($\Delta G° = 9.23$ kcal/mol) makes this pathway not feasible to the atmospheric fate of the $(CH_3)_2SCl$ adduct. The rate constant for this channel was evaluated to be 2.2×10^{-9} cm^3 molecule^{-1} s^{-1}. These results show that the principal product of this reaction in the atmosphere will be CH_3SCH_2 + HCl.

1. Introduction

Dimethyl sulfide (DMS) is a product of biodegradation of organosulfur compounds in marine environments. It was first detected in the upper levels of the oceans by Lovelock et al.[1] Since DMS has been recognized as the main natural source of sulfur in the atmosphere, a great deal of laboratory and field research has been performed to understand the mechanism of its atmospheric transformations, and excellent reviews have been published on this subject.[2−5] DMS is oxidized in the atmosphere to form SO_2, sulfuric, acid and methanesulfonic acid (MSA) aerosol (non sea salt sulfate, NSS$-SO_4^{2-}$), and it seems to be the major source of cloud condensation nuclei (CCN) over the oceans.[6] Due to the fact that the reflectance of clouds (albedo) is sensitive to CCN density, the production of these non sea salt sulfate aerosols may provide a means of biological climate regulation, as well as contribute to the acidity of precipitation.[6]

The importance of the presence of the DMS and its trajectory in the upper atmosphere have led to several studies aiming to understand the chemistry of this compound and its oxidation products. Today, there is an overall agreement that the mechanism of its oxidation is mainly affected by OH radicals[7−9] and, in a minor extension, by NO_3[10,11] and Cl[12,13] radicals. A mechanism of the tropospheric destruction of DMS was proposed by Yin et al. in 1990,[5] using 354 reactions to model this process. However, most reaction constant data involving sulfur species used in the kinetic model were estimated, rather than based on direct experimental measurements. So, several studies have been reported on this subject, mainly because there is a number of complications that plague the experimental kinetics approaches used, and measurement of some intermediates and reactants is accessed only indirectly.

Now it is believed that the first step toward the oxidation of the DMS is the reaction with OH radical during daytime and reaction with NO_3 at night. There is a general agreement that in the absence of oxygen, the reaction that takes place is the abstraction of a hydrogen atom. On the other hand, in the presence of O_2, the reaction is the addition of OH to the sulfur atom followed by the adduct reaction with O_2. Nevertheless, no direct spectroscopic observation of the DMS···OH adduct has been reported, showing that this path deserves more attention. Theoretical studies[14] located a stable adduct only at the MP2/6-31G(d) level of calculation. At the MP2/6-31+G-(2d) level, the complex is bound by 9.3 kcal/mol. Recent experimental results[15] indicate that this adduct is more stable in aqueous phase than in gaseous phase, suggesting that the rate and mechanism of the OH-initiated atmospheric destruction of DMS may depend considerably on the presence or not of water droplets. In addition, some field measurements of the SO_2 concentrations[16] and model calculations[17] suggest that the production of SO_2 in the atmospheric oxidation of DMS is lower than that predicted earlier. Recently, an uncertainty and sensitivity analysis[18] was performed to evaluate the OH-initiated DMS oxidation kinetics, and the results suggested that some kinetic parameters currently in use deserve a more accurate determination.

Thus, the information resulting from studies reported so far are not sufficient to explain the entire mechanism, the products, and the quantities observed. In addition, field studies of sulfur marine chemistry seem to suggest that the DMS removal is too rapid to be accounted for entirely by reactions with OH and

[⊗] Abstract published in *Advance ACS Abstracts,* December 1, 1997.

S1089-5639(97)01885-9 CCC: $14.00

NO_3 species.[13] Therefore, other alternative initiation reactions involving different species were suggested,[19] and other mechanisms involving intermediates such as $CH_3SCH_2O_2$,[20] CH_3SCHO,[21] CH_3S, and CH_3SO_x[22,23] have been investigated. One interesting possibility is the initial reaction of DMS with Cl radicals. Recently, it has been suggested that the atmospheric concentration of Cl atoms in the marine atmosphere could be significant compared with the atmospheric concentration of OH.[24] Considering the great reactivity of Cl atoms with organic molecules, it was estimated that if the Cl atmospheric concentration reaches 10^4 molecules/cm^3, the rates of removal of DMS by Cl and OH would become competitive.[13] The more accepted source of atmospheric atomic chlorine seems to be $ClNO_2$, which is generated by heterogeneous reaction of N_2O_5 vapor with moist NaCl.[13]

Four channels are possible for the reaction of Cl with DMS (reaction 1):

$$Cl + CH_3SCH_3 \rightarrow (CH_3)_2SCl \quad (1a)$$

$$\rightarrow CH_3SCH_2 + HCl \quad (1b)$$

$$\rightarrow CH_3S + CH_3Cl \quad (1c)$$

$$\rightarrow CH_3SCl + CH_3 \quad (1d)$$

Nielsen et al.[25] have determined the rate constants for the reactions of OH and Cl with dimethyl sulfide and other sulfur-reduced compounds. The chlorine atom rate constants were measured using photolysis of phosgene to produce Cl atoms, and the reaction was monitored and analyzed by gas chromatography. The value obtained for the DMS + Cl reaction was $(32.2 \pm 3) \times 10^{-11}$ cm^3 molecule^{-1} s^{-1}.

Stickel et al.[13] have studied this reaction using laser flash photolysis of $Cl_2CO/DMS/N_2$ mixtures with time-resolved analysis of Cl atoms by resonance fluorescence. Their results showed that the reaction between Cl and DMS is very fast, occurring on essentially every encounter of these species. They have also observed that the reaction rate increases with the decrease of temperature and shows significant pressure dependence. At 298 K, the rate constant was determined to be $(3.3 \pm 0.5) \times 10^{-10}$ cm^3 molecule^{-1} s^{-1} at 700 Torr and 1.8×10^{-10} cm^3 molecule^{-1} s^{-1} in the low-pressure limit. This result and the heat of formation estimate of the products for the four channels described above led to the conclusion that the hydrogen abstraction, channel 1b, is the dominant reaction pathway in the limit of low pressure. However, the channel 1a becomes competitive at higher pressure. Stickel et al.[13] also estimated the reaction heats for every channel, which are compared with our results.

Using a discharge-flow reactor coupled to a mass spectrometer, Butkovskaya et al.[26] have studied the same reaction at 298 K and 1 Torr and confirmed that it proceeds only through the channel 1b, giving CH_3SCH_2 and HCl.

The tunable diode laser absorption spectroscopy (TDLAS) technique was used by Zhao et al.,[27] to follow the temporal evolution of the CH_3 concentration after a flash photolysis has produced Cl in a gas mixture containing $COCl_2$ and DMS. Their measurements showed that the CH_3 yields for this reaction are very small, and they have suggested that this could be removed from the list of possible fates of the $(CH_3)_2SCl$ adduct.

Kinnison et al.[12] have also determined the rate coefficients for reaction 1, monitoring by gas chromatography the decay of the sulfide occurred as a result of the reaction with chlorine atoms generated by photolysis of the $COCl_2$. The experiments were conducted in atmospheres of N_2 and synthetic air, to investigate the influence of the presence of oxygen on the rate coefficient. The results showed that the rate coefficient is affected by the oxygen, and the values obtained were 3.61×10^{-10} cm^3 molecule^{-1} s^{-1} in inert atmosphere and $(4.03 \pm 017) \times 10^{-10}$ cm^3 molecule^{-1} s^{-1} in synthetic air. It suggests that the $(CH_3)_2SCl$ adduct react with O_2, which reduces the backward reaction and leads to a net increase of the rate coefficient of the channel 1a.

The yield of the CH_3Cl in the DMS + Cl reaction was assessed in experiments carried out by Langer et al.[28] They have measured a small yield of $(1.34 \pm 0.07) \times 10^{-3}$ for CH_3Cl and verified an independence of this value of the initial reactant concentrations and of the extent of reaction, which suggest that it is not formed in secondary reactions. They concluded that the source of the CH_3Cl is the decomposition of the $(CH_3)_2SCl$ adduct but have not found an explanation for the high CH_3Cl concentration measured recently over the Labrador Sea.

The only theoretical study reported on this system was performed by McKee.[14] It was found that the $(CH_3)_2SCl$ adduct is stable by 12.8 kcal/mol at the PMP2/6-31G(d) single-point calculations using the UHF/6-31G(d) level of geometry optimization. However, the overall mechanism of the adduct formation and decomposition was not studied.

The experimental studies reported so far show that the channels 1a and 1b are the most significant in the reaction of the Cl with DMS. However, the energetics of the pathways 1c and 1d are not sufficiently known, and we believe that a theoretical study of this system can be of great aid in the comprehension of the mechanism and kinetics involved in the process of the oxidation of the DMS and the $(CH_3)_2SCl$ adduct in the marine atmosphere. In this work, we have performed ab initio calculations to determine the mechanism of the reaction of Cl with DMS and have calculated the activation and reaction energies for every one of the four possible channels presented above. The energetic, kinetic, and thermodynamic features of this reaction were analyzed, and the atmospheric implications of our results are discussed.

2. Calculations

The calculations were performed using the Gaussian 94[29] and GAMESS[30] suites of programs. We have performed geometry optimizations at the UMP2(fc)/DZP level of theory. The DZP basis set is a contraction of (9s5p1d)/[4s2p1d] for the first-row atoms and (11s7p1d)/[6s4p1d] for the second-row atoms.[31] The polarization exponents used are 0.75 (carbon), 1.0 (hydrogen), 0.532 (sulfur), and 0.6 (Cl). Single-point energy calculations for the optimized stationary points were carried out using RMP2,[32] UMP4(SDTQ), and UQCISD(T) methods. The projected values for the spin contamination S^2 and UMP2 energies (PMP2)[33] were also considered. We have also included the results for the projected UMP4 values calculated using the following approximate formula proposed by Chen and Schlegel[34]

$$E_{\mathrm{PUMP4}} = E_{\mathrm{PUMP3}} + E_4$$

where E_4 is the difference between the E_{UMP4} and E_{UMP3} values. We are interested in evaluating the accuracy of this approach for the system studied here, by comparison of the results with the UQCISD(T) calculations.

The absolute energies for all stationary points and their respective frequencies are in Table 1. The $(CH_3)_2SCl$ adduct obtained by McKee[14] was fully optimized, and we have

TABLE 1: Absolute Energies (in hartrees) and Frequencies (in cm^{-1}) Obtained for All Stationary Points Obtained in This Work, at the UMP2/DZP Level of Theory

species	energy/hartrees	frequencies/cm^{-1}
CH_3SCH_3	−477.177 252 6[a]	164, 193, 271, 738, 792, 938, 982, 1022, 1080, 1391, 1419, 1495, 1507, 1519, 1528, 3106, 3110, 3216, 3222, 3237, 3238
Cl	−459.550 791 3	
adduct 1	−936.751 551 2	112, 167, 168, 187, 282, 300, 735, 791, 953, 982, 1015, 1086, 1387, 1411, 1490, 1497, 1504, 1509, 3124, 3127, 3250, 3253, 3264, 3266
adduct 2	−936.729 058 3	18, 23, 37, 158, 189, 271, 739, 792, 937, 979, 1020, 1078, 1388, 1417, 1487, 1504, 1517, 1527, 3108, 3113, 3217, 3224, 3239, 3243
adduct 3	−936.728 317 6	14i, 23, 27, 160, 190, 270, 737, 791, 937, 981, 1022, 1079, 1390, 1418, 1495, 1507, 1518, 1527, 3107, 3111, 3217, 3224, 3238, 3239
adduct 4	−936.729 240 5	11i, 40, 43, 176, 190, 270, 737, 792, 939, 1011, 1021, 1081, 1391, 1419, 1479, 1502, 1515, 1524, 3110, 3114, 3209, 3239, 3240, 3245
adduct 5	−936.728 888 2	5i, 20, 41, 162, 193, 271, 738, 791, 939, 982, 1023, 1080, 1391, 1419, 1495, 1507, 1519, 1528, 3107, 3111, 3217, 3224, 3239, 3244
MS1	−936.732 680 5	60, 66, 111, 137, 295, 304, 376, 478, 693, 748, 880, 940, 1003, 1067, 1400, 1460, 1504, 1523, 2843, 3125, 3219, 3249, 3256, 3355
TS2	−936.679 881 3	1174i, 61, 103, 113, 167, 236, 271, 755, 953, 1000, 1035, 1063, 1108, 1400, 1433, 1442, 1485, 1514, 3109, 3191, 3224, 3234, 3388, 3398
MS2	−936.742 272 9	24, 39, 42, 54, 70, 73, 757, 781, 803, 900, 1050, 1053, 1392, 1426, 1448, 1512, 1518, 1524, 3106, 3153, 3214, 3239, 3283, 3285
TS3	−936.693 871 3	389i, 111, 123, 150, 192, 279, 424, 503, 569, 755, 929, 1007, 1011, 1399, 1461, 1473, 1491, 1517, 3127, 3176, 3250, 3258, 3362, 3374
MS3	−936.702 806 6	19, 32, 45, 64, 91, 112, 208, 250, 503, 536, 751, 1006, 1012, 1398, 1466, 1466, 1486, 1520, 3119, 3206, 3241, 3254, 3412, 3413
CH_3SCH_2	−476.520 612 7	134, 241, 300, 438, 751, 870, 934, 999, 1060, 1399, 1469, 1502, 1523, 3122, 3242, 3244, 3252, 3383
HCl	−460.204 463 5[a]	3088
CH_3	−39.698 021 2	452, 1466, 1467, 3212, 3418, 3419
CH_3SCl	−897.002 734 2[a]	209, 248, 539, 751, 1006, 1011, 1400, 1483, 1521, 3117, 3237, 3255
CH_3S	−437.360 644 3	626, 759, 900, 1392, 1435, 1518, 3109, 3216, 3238
CH_3Cl	−499.378 977 8[a]	786, 1055, 1055, 1439, 1522, 1522, 3148, 3278, 3278

[a] Calculations at MP2/DZP level.

TABLE 2: Energy Values (in kcal/mol) for the DMS···Cl Adducts in Relation to DMS and Cl Atom Energy[a]

	adduct				
	1	2	3	4	5
E_{UMP2}	−14.75	−0.64	−0.17	−0.75	−0.53
E_{PUMP2}	−15.58	−0.64	−0.17	−0.76	−0.53
E_{RMP2}	−15.47	−0.61	−0.17	−0.73	−0.51
$E_{UMP4(SDTQ)}$	−13.17	−0.65	−0.16	−0.75	−0.53
E_{PUMP4}[b]	−13.63	−0.66	−0.16	−0.75	−0.53
$E_{UQCISD(T)}$	−13.31	−0.65	−0.15	−0.75	−0.52
UMP2 projected S^2	0.752	0.75	0.75	0.75	0.75
ZPE contribution	0.991	0.080	0.060	0.165	0.103

[a] The single-point energy calculations were performed with the DZP basis set in the geometries obtained at the UMP2/DZP level. [b] Values calculated using Chen and Schlegel's formula.[34]

TABLE 3: Energy Values (in kcal/mol) for the Transitions States and Intermediates of the Reaction between DMS and Cl Atom in Relation to Reactants[a]

	MS1	TS2	MS2	TS3	MS3
E_{UMP2}	−2.91	30.22	−8.93	21.44	15.84
E_{PUMP2}	−3.63	23.45	−9.16	17.99	15.47
E_{RMP2}	−3.11	29.20	−8.96	21.97	16.05
$E_{UMP4(SDTQ)}$	−1.98	29.33	−8.59	21.08	15.83
E_{PUMP4}[b]	−2.54	24.36	−8.77	18.31	15.47
$E_{UQCISD(T)}$	−2.96	26.43	−8.84	18.86	15.44
projected S^2	0.754	0.849	0.751	0.806	0.753
ZPE contribution	−2.966	−0.691	−0.601	−1.755	−3.654

[a] The single-point energy calculations were performed with the DZP basis set in the geometries obtained at the UMP2/DZP level. [b] Values calculated using Chen and Schlegel's formula.[34]

investigated the stability of the Cl atom at several positions around the DMS. One other minimum energy adduct and three first-order transition states were located. The geometric parameters for all adducts obtained are shown in Figure 1. The energy values in relation to reactants are given in Table 2.

TABLE 4: Energy Values (in kcal/mol) for the Products of the Reaction between DMS and Cl Atom in Relation to Reactants[a]

	$CH_3SCH_2 + HCl$	$CH_3S + CH_3Cl$	$CH_3 + CH_3SCl$
E_{UMP2}	1.86	−7.27	17.12
E_{PUMP2}	1.11	−7.48	16.74
E_{RMP2}	1.72	−7.31	17.35
E_{UMP4}	2.39	−6.92	17.09
E_{PUMP4}[b]	1.80	−7.09	16.73
$E_{UQCISD(T)}$	1.41	−7.19	16.67
projected S^2	0.755	0.751	0.753
ZPE contribution	−4.598	−1.274	−4.225

[a] The single-point energy calculations were performed with the DZP basis set in the geometries obtained at the UMP2/DZP level. [b] Values calculated using Chen and Schlegel's formula.[34]

We have studied the four channels suggested above for the reaction 1. The transition states for the reactions were characterized via harmonic frequency analysis and connected to the respective minimum energy structures through IRC (intrinsic reaction coordinate) calculations, following the Gonzalez and Schlegel implementation.[35] The stationary points located on the potential energy surface for this reaction are represented in Figure 2, and Table 3 gives the energies relative to reactants. For the 1b channel, the hydrogen abstraction occurs without barrier, leading to a van der Waals complex between the products, CH_3SCH_2 radical and HCl. For 1c and 1d pathways the reaction involves the formation of a transition state followed by a van der Waals complex before decomposition into the products, $CH_3S + CH_3Cl$ and $CH_3SCl + CH_3$.

Table 4 reports the relative energies for the products in relation to reactants, and Figure 3 shows the optimized geometries of the DMS and products. The relative energies including ZPE (zero-point energy) contribution and the thermodynamic values are shown in Table 5, for the four channels discussed above.

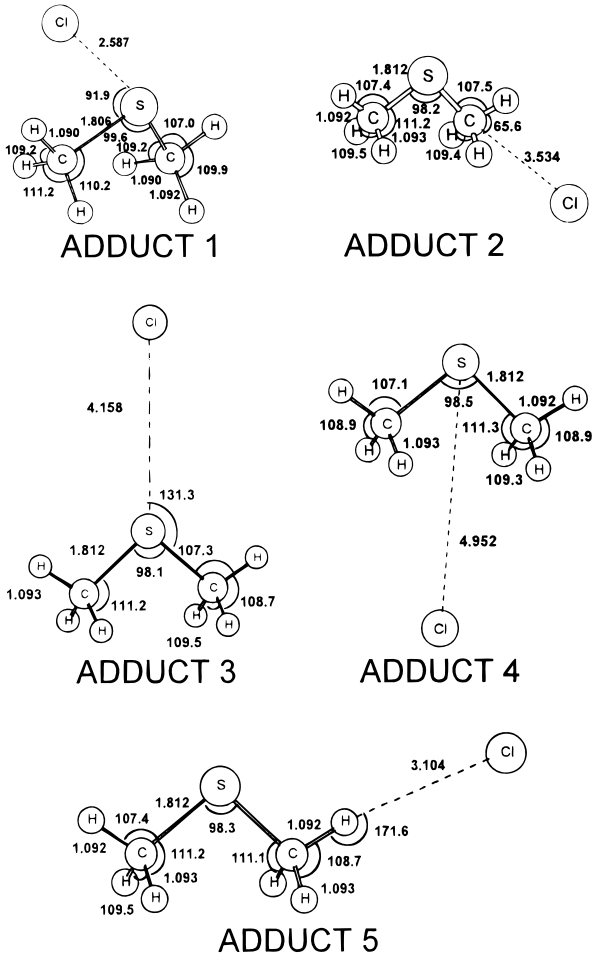

Figure 1. Molecular structures and geometrical parameters for the adducts of DMS and Cl atom obtained at the UMP2/DZP level of calculation. Adducts 1 and 2 are minimum energy structures, and adducts 3, 4, and 5 are first-order transition states.

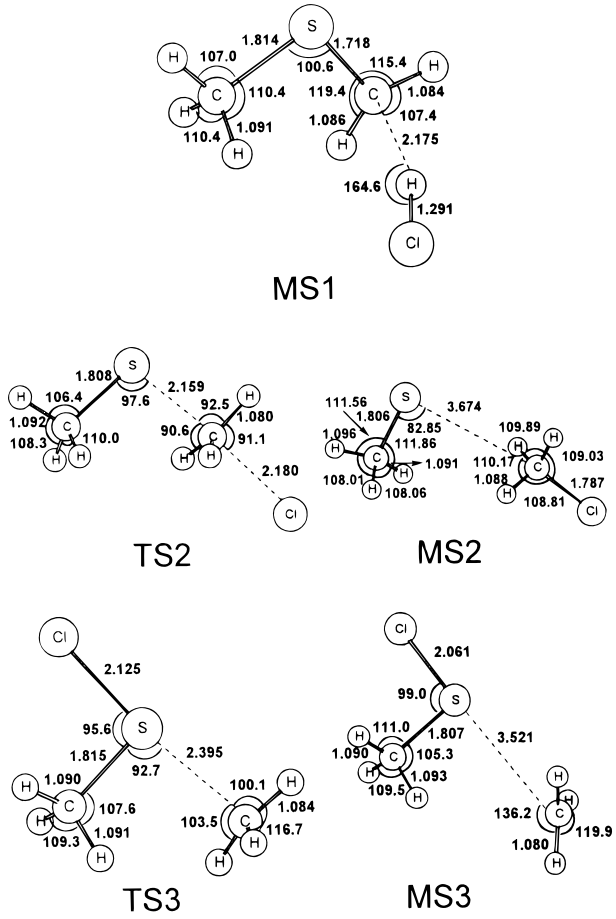

Figure 2. Molecular structures and geometrical parameters for the intermediates and transition states obtained at the UMP2/DZP level of calculation for the reaction between DMS and Cl atom.

3. Discussion

Observing the energetic values obtained for the five adducts of DMS with Cl atom using higher level correlated methods, it can be seen that convergence is reached with the UQCISD(T) calculation with the basis set employed. In fact, with a UMP4-(SDTQ) calculation, the principal features of the correlation are included, and the PUMP4 values do not present significant differences. The projected S^2 values for the UMP2 wave function show that there is no spin contamination.

Adducts 1 and 2 are minimum energy complexes, and adducts 3, 4, and 5 are first-order transition states, with imaginary frequencies of 14i, 11i, and 5i, respectively. Adduct 3 is the transition state for the interconversion of the chlorine atom from one to the other side of the DMS. The barrier for this motion was calculated to be 12.23 kcal/mol, at the UQCISD(T)/DZP//MP2/DZP level including ZPE contribution. Although this is not a very high barrier, it should be noted that this complex is stable in relation to monomers by ca. 0.2 kcal/mol, and the S−Cl interatomic distance is ca. 4 Å. It is possible that the weak adduct 3 would not be predicted to exist using a higher level calculation. In fact, except for adduct 1, which is bound through the lone pair of the S atom, all adducts are very weakly bound, with stabilization energies lower than 1 kcal/mol. Thus, they do not play an important role in the reaction between DMS and Cl atom. The precise identification of the nature of these weakly bound adducts could be reached with a better level of calculation. However, our present computational resources preclude such calculations to be performed in our laboratory.

The results reported in Table 3 show that the projection of the UMP2 energies leads to a stabilization of the species, in relation to reactants. The same behavior is verified in the results for the projection of UMP4 energies, using the Chen and Schlegel formula. The RMP2 results do not show a regular tendency, presenting lower relative energies than the UMP2 values for MS1, TS2, and MS2 stationary points, but show higher relative energies for the other species (TS3 and MS3). The relative UQCISD(T) energies are always lower than the UMP2 energies, except for MS2, where the difference is very small. A comparison between the PUMP4 and the UQCISD-(T) energies shows that the Chen and Schlegel approach is better to correct the energies of the minimum states than the transition states. This procedure leads to overstabilization of the transition states. It can also be observed that the projected S^2 values are very satisfactory for the minimum energy structures but not so good for the transition states.

The structure of adducts 2 and 5 and MS1 show that these species have different interactions between the chlorine atom and the DMS. Depending on the position of the chlorine atom, the interaction with a hydrogen or carbon atom of DMS can lead to the formation of distinct species: a very weakly bound complex (adduct 5), a complex that will lead to a reaction where the break of a C−S bond takes place (adduct 2), or to the abstraction of the hydrogen, forming a complex between HCl and CH_3SCH_2 (MS1). The MS1 species is a result of the attack of the chlorine atom to the lateral hydrogens. In this case, the reaction occurs without barrier, and there is no adduct formation where the chlorine atom interacts with one of the lateral hydrogens. It is in contrast with the formation of adduct 5,

TABLE 5: Energies in Relation to Reactants Including ZPE Contribution (ΔE) and Thermodynamic Results at 298.15 K and 1 atm for Every Channel Considered in the Reaction between DMS and Cl Atom, Computed at the UQCISD(T)//UMP2/DZP Level of Calculation[a]

	ΔE/kcal·mol^{-1}	ΔH/kcal·mol^{-1}	ΔG/kcal·mol^{-1}	ΔS/cal·K^{-1}·mol^{-1}	ΔH/kcal·mol^{-1} (ref 13)[a]
adduct 1	−12.32	−12.72	−5.63	−23.78	-14 ± 3
MS1	−5.96	−5.65	−0.69	−16.64	
$CH_3SCH_2 + HCl$	−3.19	−2.50	−5.33	9.49	-8 ± 2
TS2	25.74	25.58	31.45	−19.69	
$CH_3S + CH_3Cl$	−8.46	−8.55	−12.13	12.01	-9.8 ± 0.5
TS3[b]	29.43	29.59	29.25	1.14	
$CH_3SCl + CH_3$	12.45	13.12	9.23	13.05	8 ± 4

[a] The last column shows the estimations of Stickel et al.[13] [b] Values relative to adduct 1.

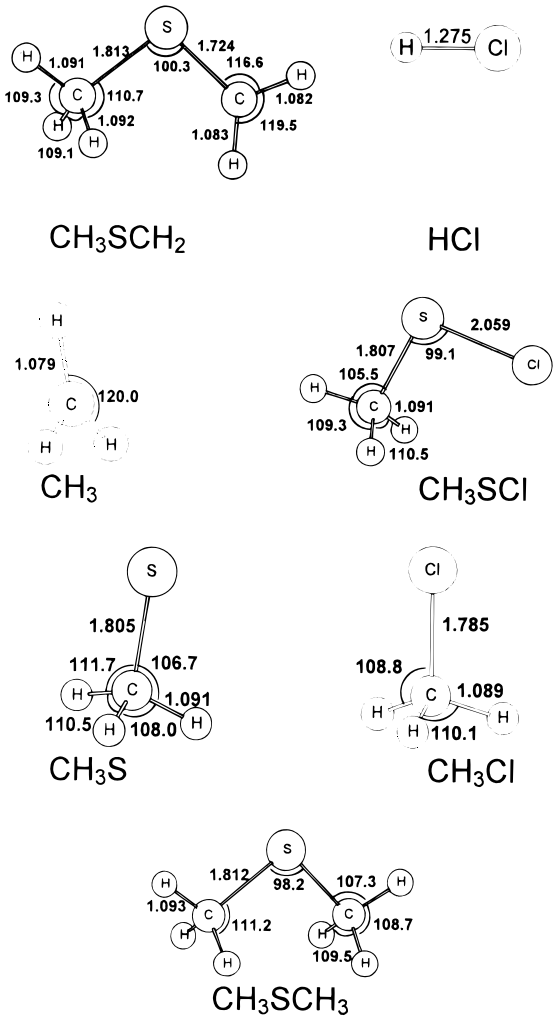

Figure 3. Molecular structures and geometrical parameters for the products of the reaction between DMS and Cl atom and for DMS, at the UMP2/DZP level of calculation.

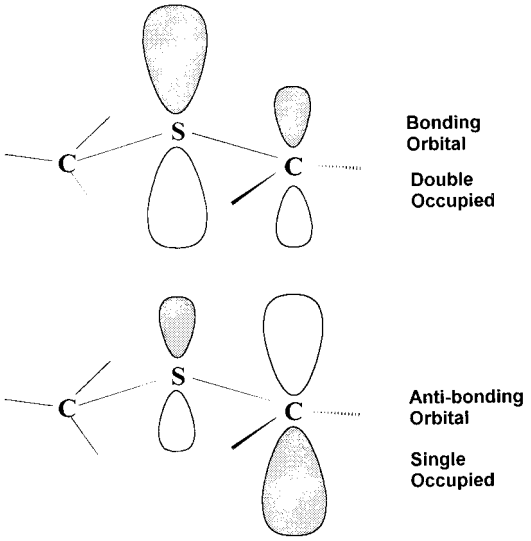

Figure 4. Schematic representation of the π molecular orbitals of the S−C bond in the CH_3SCH_2 radical.

where there is a barrier to the hydrogen abstraction. This difference in the behavior can be understood observing the orbital structure of the CH_3SCH_2 radical showed in Figure 4. This figure shows the bonding (HOMO, highest occupied molecular orbital) and antibonding π orbitals (SOMO, single occupied molecular orbital) resulting of the combination of the single occupied p orbital of the carbon and the double occupied p orbital of the sulfur atom. This orbital arrangement leads to a radical species where the two remaining hydrogens, the carbon, and the sulfur atoms are almost planar. It also provides a justification for the interaction of the chlorine atom with the lateral hydrogens (leading to reaction 1b) to be different from that with the superior hydrogen (leading to adduct 5). The interaction that leads to channel 1b is very favorable because the hydrogen atom departs leading to an almost planar structure due to an effective overlap between the atomic orbitals of the carbon and sulfur atoms. The depart of the superior hydrogen of the DMS result in a unstable conformation of the CH_3SCH_2 radical, which will require a rotation of CH_2 group to reach the almost planar structure.

A similar tendency of the results reported in Table 3 can be verified in the values given in Table 4. The projection also leads to a decrease of the relative energy of the products at UMP2 and UMP4 levels. For the values given in Table 4, the relative UQCISD(T) energies are lower than the UMP2 values only for the products of the 1b and 1d channels but are always lower than the relative PUMP4 energies. Here, the PUMP4 approach also has the tendency to bring the UMP4 results near to the UQCISD(T) values. The unique product that is less stable than the reactants, including the ZPE contribution, is the $CH_3 + CH_3SCl$, channel 1d. The projected S^2 values for CH_3SCH_2, CH_3S, and CH_3 radicals are also very good.

Figure 5 shows a relative energy diagram for the four channels involved in this reaction at the UQCISD(T)/DZP//UMP2/DZP level of calculation plus ZPE contribution. The values obtained for the four different channels of the reaction between DMS and Cl atom indicate that the principal paths are the 1a and 1b channels. The 1a channel leads to formation of the $(CH_3)_2SCl$ adduct, which is stable by 12.32 kcal/mol in relation to reactants.

The 1b channel is the abstraction reaction that leads to CH_3SCH_2 and HCl. There is no energy barrier for the formation of a weakly bound molecular complex between these two species. The stabilization energy in relation to reactants is −5.92 kcal/mol. The products are only 2.73 kcal/mol above this complex and 3.19 kcal/mol below the reactants.

The 1c channel encompass the formation of a molecular complex (adduct 2) stabilized by 0.57 kcal/mol, which then

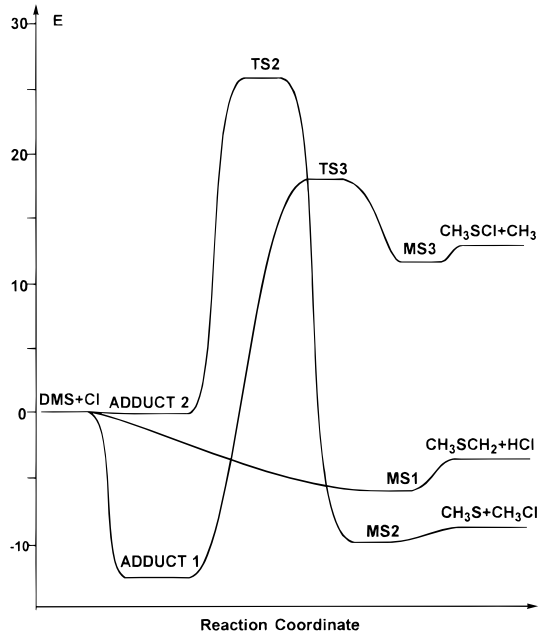

Figure 5. Energy diagram for the reaction between DMS and Cl atom, evaluated using the UQCISD(T)//UMP2/DZP level of calculation with inclusion of the ZPE contribution.

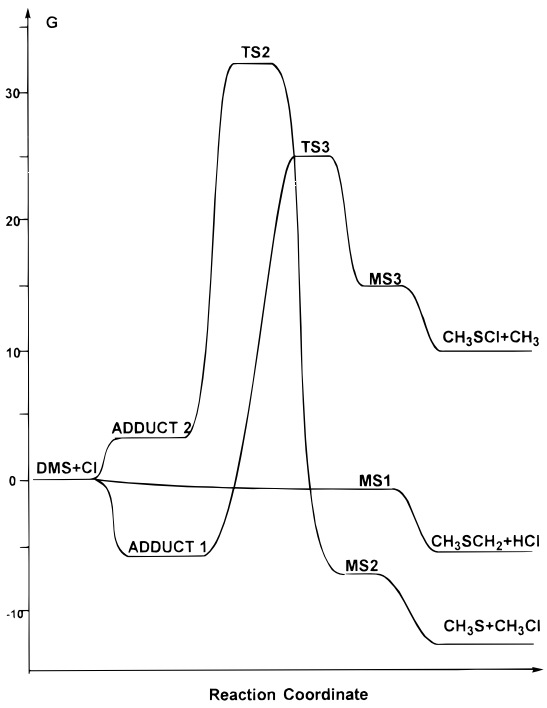

Figure 6. Energy diagram for the variation of Gibbs free energy in the reaction between DMS and Cl atom. Calculations were performed at UMP2/DZP level of calculation.

requires 26.31 kcal/mol to reach the transition state TS2. This transition state goes to a molecular complex (MS2) with stabilization energy of 9.44 kcal/mol in relation to reactants, which needs an additional 0.98 kcal/mol to dissociate into the CH_3Cl and CH_3S products. Although these products are more stable than the reactants by 8.46 kcal/mol, this path has a high activation energy barrier, and it is not very feasible in principle.

The last channel, the formation of CH_3SCl and CH_3 radical, is only accessed through the adduct 1. The transition state TS3 can be formed with an energy of 29.43 kcal/mol above the adduct 1, and then it goes to a weakly bound minimum energy complex, MS3. This molecular complex is 11.79 kcal/mol above the reactants but is 4.32 kcal/mol less energetic than the transition state. It requires only 0.66 kcal/mol for the dissociation of the MS3 complex into CH_3SCl and CH_3. This channel is also not favorable, because it involves a very energetic transition state, TS3, and the products are less stable than the reactants by 12.45 kcal/mol.

By analyzing the thermodynamic data in Table 5, it can be seen that our ΔH results are in good agreement with the values estimated by Stickel et al., except for the channel 1b. This behavior is owing to the CH_3SCH_2 heat of formation used by Stickel et al., which is much approximated. It also can be seen that 1a, 1b, and 1c channels are spontaneous ($\Delta G < 0$), but 1d is not. Figure 6 shows the Gibbs energy differences for each channel. It can be observed that the ΔG values for the channels 1a and 1b are of the same order, which means that the equilibrium constants for these two channels will be very close. These two channels do not have an activation energy barrier. The products for the channel 1c are the most stable ones, but the activation free energy in relation to reactants ($\Delta G^{\ddagger} = 31.45$ kcal/mol) is the largest, which renders this reaction to be not viable in principle. The activation free energy to channel 1d is also very high, $\Delta G^{\ddagger} = 29.25$ kcal/mol, and the products are less stable than reactants.

The equilibrium constants for the channels 1a and 1b were calculated and are, respectively, 3.29×10^5 and 1.98×10^5 L/mol. Assuming that the concentration of chlorine is 10^4 molecule^{-1}/cm^3 and the concentration of DMS is 3×10^{-9} mol/L,[36,37] the equilibrium concentrations of HCl and CH_3SCH_2 are calculated as 1×10^{-10} mol/L, but the concentration of the adduct will be approximately 2×10^{-20} mol/L. Therefore, channel 1a will reach equilibrium very fast, and the concentration of the product will be very small, while the channel 1b will be the main pathway responsible for the reaction of chlorine atoms with DMS.

Using the ΔG values for the channels 1c and 1d, we have estimated the reaction rate constants for these pathways to be 2.1×10^{-30} cm^3 molecule^{-1} s^{-1} for channel 1c and 2.2×10^{-9} s^{-1} for channel 1d. The rate constants for the channels 1a and 1b will be very large because these channels do not have activation energy. Therefore, we can conclude that kinetically governed processes, occurring in a short scale time, will be following practically only these two pathways. These results are in agreement with the kinetically experimental previsions of Stickel et al.,[13] who suggested that the H-abstraction pathway accounts for about 40−50% of the overall reaction between DMS and chlorine atom in atmospheric pressure (700 Torr), with the adduct formation apparently becoming competitive. Although channel 1c presents the more stable products, it is the slowest reaction, and the CH_3S and CH_3Cl products should not be observed in kinetic studies that are conducted on a very short scale time.

4. Atmospheric Implications

Our results show that the main products for the reaction between DMS and Cl atoms will be the $(CH_3)_2SCl$ adduct, CH_3SCH_2, and HCl, that means that the channels 1a and 1b will be favored in terms of kinetics. Channel 1a has a small thermodynamic preference over 1b channel, and in kinetics experiments that are realized on a short time scale, these two channels will be significant. However, under atmospheric conditions, pathway 1a rapidly reaches equilibrium, and the concentrations of adduct 1 will be very small. Therefore, channel 1b will be the most important to the reaction between DMS and chlorine atoms in the atmosphere.

Nevertheless, one of the products of channel 1c (CH_3Cl) was observed in the experimental work of Langer et al.,[28] and

exceptional concentrations of CH_3Cl were detected in the region of the Labrador Sea. Despite the fact that the products of channel 1c are the most stables and the reaction is thermodynamically possible, this pathway is much hindered kinetically. According to our calculations, the direct formation of CH_3Cl and CH_3S (channel 1c) will not occur, and we believe that these products could be formed through other pathways. A possibility is the presence of another species besides DMS and Cl, which could stabilize both the adduct and the transition state involved in this pathway. Langer et al. also suggested that the CH_3Cl could be formed from CH_3 produced in channel 1d. However, we have shown that the path for direct formation reaction of CH_3 is as hindered as the path for the direct formation reaction of CH_3Cl, and it is thermodynamically unfavorable.

Another interesting fact is that the path to channel 1d is conditional to the formation of the adduct 1, $(CH_3)_2SCl$. However, it cannot be considered a possible fate for this adduct because of the high activation energy involved, and the formation of the CH_3SCl and CH_3 products will be negligible. In fact, the decomposition of the $(CH_3)_2SCl$ adduct in atmospheric conditions will not be important because its concentration will be very small. However, there is a possibility of this adduct to be stabilized by another species, as occurs with the adduct between DMS and OH, which is stabilized by O_2. More research is necessary to access the stability of the interaction of the $(CH_3)_2SCl$ adduct with other species, and we are investigating these processes.

5. Conclusions

The reaction between dimethyl sulfide and chlorine atom was studied theoretically in order to assess the feasibility of this reaction. We have calculated the activation and reaction energies for every step and evaluated the thermodynamic properties such as Gibbs free energies, entropies and enthalpies. We have concluded that the reaction will follow preferentially channels 1a and 1b, with a small advantage for channel 1a in kinetics experiments. However, in atmospheric conditions channel 1b will be dominant. Channel 1c will only be significant in situations where thermodynamic equilibrium can be reached. Channel 1d proceeds with the formation of the $(CH_3)_2SCl$ adduct, but this reaction is not viable thermodynamically, and it could not be considered a possible atmospheric fate for this adduct. In fact, adduct formation does not play an important role in the atmospheric reaction between DMS and chlorine atoms if the interaction with other species does not occur. We also think that high-level ab initio calculations, as performed in this study, can be of great aid to encompass many aspects of this complex atmospheric system that is the dimethyl sulfide cycle.

Acknowledgment. The authors thank the Conselho Nacional de Desenvolvimento Científico e Tecnológico (CNPq) for providing the research grants, and the Fundação de Amparo à Pesquisa no Estado de Minas Gerais (FAPEMIG), the Programa de Apoio ao Desenvolvimento Científico e Tecnológico (PADCT—Proc No. 620241/95.0), and the Pró-Reitoria de Pesquisa (PRPq − UFMG) for supporting this project. The authors also thank Josefredo R. Pliego Jr for the helpful discussions and for reading the manuscripts.

References and Notes

(1) Lovelock, J. E.; Maggs, R. J.; Rasmussen, R. A. *Nature* **1972**, *237*, 452.

(2) Barone, S. B.; Turnipseed, A. A.; Ravishankara, A. R. *J. Chem. Soc., Faraday Trans.* **1995,** *100*, 39.

(3) Tyndall, G.; Ravishankara, A. R. *Int. J. Chem. Kinet.* **1991,** *23*, 483.

(4) Yin, F.; Grosjean, D.; Seinfeld, J. H. *J. Atmos. Chem.* **1990,** *11*, 309.

(5) Yin, F.; Grosjean, D.; Flagan, R. C.; Seinfeld, J. *J. Atmos. Chem.* **1990,** *11*, 365.

(6) Charlson, R. J.; Lovelock, J. E.; Andreae, M. O.; Warren, S. G. *Nature* **1987**, *326*, 655.

(7) Sφrensen, S.; Falbe-Hansen, H.; Mangoni, M.; Hjorth, J.; Jensen, N. R. *J. Atmos. Chem.* **1996,** *24*, 299.

(8) Barone, S. B.; Turnipseed, A. A.; Ravishankara, A. R. *J. Phys. Chem.* **1996**, *100*, 14694.

(9) Hynes, A. J.; Wine, P. H.; Semmes, D. H. *J. Phys. Chem.* **1986**, *90*, 4148.

(10) Butkovskaya, N. I.; Le Bras, G. *J. Phys. Chem.* **1994**, *98*, 2582.

(11) Jensen, N. R.; Hjorth, J.; Lohse, C.; Skov, H.; Restelli, G. *J. Atmos. Chem.* **1992,** *14*, 95.

(12) Kinnison, D. J.; Mengon, W.; Kerr, J. A. *J. Chem. Soc., Faraday Trans.* **1996,** *92*, 369.

(13) Stickel, R. E.; Nicovich, J. M.; Wang, S.; Zhao, Z.; Wine, P. *J. Phys. Chem.* **1992**, *96*, 9875.

(14) McKee, M. L. *J. Phys. Chem.* **1993**, *97*, 10971.

(15) Merényi, G.; Lind, J.; Engman, L. *J. Phys. Chem.* **1996**, *100*, 8875.

(16) Bandy, A. R.; Scott, D. L.; Blomquist, B. W.; Chen, S. M.; Thornton, D. C. *Geophys. Res. Lett.* **1992,** *19*, 1125.

(17) Lin, X.; Chameides, W. L. *Geophys. Res. Lett.* **1993,** *20*, 579.

(18) Saltelli, A.; Hjorth, J. *J. Atmos. Chem.* **1995,** *21*, 187.

(19) Cvetanovic, R. J.; Singleton, D. L.; Irwin, R. S. *J. Am. Chem. Soc.* **1981,** *103*, 3530.

(20) Wallington, T. J.; Ellermann, T.; Nielsen, O. J. *J. Phys. Chem.* **1993,** ***97***, 8442.

(21) Patroescu, I. V.; Barnes, I.; Becker, K. H. *J. Phys. Chem.* **1996**, *100*, 17207.

(22) Ray, A.; Vassalli, I.; Laverdet, G.; Le Bras, G. *J. Phys. Chem.* **1996**, *100*, 8895.

(23) Turnipseed, A. A.; Barone, S. B.; Ravishankara, A. R. *J. Phys. Chem.* **1993**, *97*, 5926.

(24) Pszenny, A. A. P.; Keene, W. C.; Jacob, D. J.; Fan, S.; Maben, J. R.; Zetwo, M. P.; Springer-Young, M.; Galloway, J. N. *Geophys. Res. Lett.* **1993,** *20*, 699.

(25) Nielsen, O. J.; Sidebotton, H. W.; Nelson, L.; Rattigan, O.; Treacy, J. J.; O'Farrell, D. J. *Int. J. Chem. Kinet.* **1990,** *22*, 603.

(26) Butkovskaya, N. I.; Poulet, G., Le Bras; G. *J. Phys. Chem.* **1995**, *99*, 4536.

(27) Zhao, Z.; Stickel, R. E.; Wine, P. H. *Chem. Phys. Lett.* **1996,** *251*, 59.

(28) Langer, S.; McGovney, B. T.; Finlayson-Pitts, B. J. *Geophys. Res. Lett.* 1996, *23*, 1661.

(29) Frisch, M. J.; Trucks, G. W.; Schlegel, H. B.; Gill, P. M. W.; Johnson, B. G.; Robb, M. A.; Cheeseman, J. R.; Keith, T.; Petersson, G. A.; Montgomery, J. A.; Raghavachari, K.; Al-Laham, M. A.; Zakrzewski, V. G.; Ortiz, J. V.; Foresman, J. B.; Cioslowski, J.; Stefanov, B. B.; Nanayakkara, A.; Challacombe, M.; Peng, C. Y.; Ayala, P. Y.; Chen, W.; Wong, M. W.; Andres, J. L.; Replogle, E. S.; Gomperts, R.; Martin, R. L.; Fox, D. J.; Binkley, J. S.; Defrees, D. J.; Baker, J.; Stewart, J. P.; Head-Gordon, M.; Gonzalez, C.; Pople, J. A. *Gaussian 94*, Revision D.2; Gaussian, Inc.: Pittsburgh PA, 1995.

(30) Schmidt, M.; Baldridge, K.; Boatz, J.; Elbert, S.; Gordon, M.; Jensen, J.; Koseki, S.; Matsunaga, N.; Nguyen, K.; Su, S. J.; Windus, T.; Dupuis, M.; Montgomery, J. GAMESS. *J. Comput. Chem.* **1993,** *14*, 1346.

(31) Dunning Jr, T. H.; Hay, P. J. In *Modern Theoretical Chemistry*; Schaefer, H. F., III, Ed.; Plenum: New York, 1976; Chapter 1.

(32) Knowles, P. J.; Andrews, J. S.; Amos, R. D.; Handy, N. C.; Pople, J. A. *Chem. Phys. Lett.* **1991,** *186*, 130.

(33) McDouall, J. J. W.; Schlegel, H. B. *J. Chem. Phys.* **1989,** *90*, 2363.

(34) Chen, W.; Schlegel, H. B. *J. Chem. Phys.* **1994,** *101*, 5957.

(35) Gonzalez, C.; Schlegel, H. B. *J. Phys. Chem.* **1990,** *94*, 5523.

(36) Koga, S.; Tanaka, H. *J. Atmos. Chem.* **1996**, *23*, 163.

(37) Andreae, M. O.; Raemdonck, H. *Science* **1982**, *221*, 744.